Journal of Applied Polymer Science

Ultralight and hydrophobic nanofibrillated cellulose aerogels from coconut shell with ultrastrong adsorption properties

Caichao Wan,[1] Yun Lu,[2] Yue Jiao,[1] Chunde Jin,[3] Qingfeng Sun,[3] Jian Li[1]

[1]Material Science and Engineering College, Northeast Forestry University, Harbin 150040, China
[2]Research Institute of Wood Industry, Chinese Academy of Forestry, Beijing 100091, China
[3]School of Engineering, Zhejiang Agricultural and Forestry University, Lin'an 311300, China
Correspondence to: Y. Lu (E-mail: luyun@criwi.org.cn), Q. Sun (E-mail: qfsun@nefu.edu.cn), and J. Li (E-mail: nefulijian@163.com)

ABSTRACT: Ultralight aerogels based on nanofibrillated cellulose (NFC) isolated from coconut shell were successfully prepared via a mild fast method, which included chemical pretreatment, ultrasonic isolation, solvent exchange, and *tert*-butanol freeze drying. The as-prepared NFC aerogels with complex three-dimensional fibrillar networks had a low bulk density of 0.84 mg/cm^3 (specific surface area = 9.1 m^2/g and pore volume = 0.025 cm^3/g), maintained a cellulose I crystal structure, and showed more superior thermal stability than the coconut shell raw materials. After the hydrophobic modification by methyl trichlorosilane (MTCS), the NFC aerogels exhibited high water repellency properties, an ultrastrong oil-adsorption capacity (542 times that of the original dry weight of diesel oil), and superior oil–water separation performance. Moreover, the absorption capabilities of the MTCS-treated NFC aerogels were as high as 296−669 times their own weights for various organic solvents and oil. Thus, this class of high-performance adsorbing materials might be useful for dealing with chemical leaks and oil spills. © 2015 Wiley Periodicals, Inc. J. Appl. Polym. Sci. **2015**, *132*, 42037.

KEYWORDS: adsorption; cellulose and other wood products; functionalization of polymers; nanostructured polymers; surfaces and interfaces

Received 18 July 2014; accepted 30 January 2015
DOI: 10.1002/app.42037

INTRODUCTION

Cellulose aerogels, which are green biodegradable nanoporous materials, combine the excellent properties of traditional silica aerogels and hydrocarbon copolymers or polymer-based aerogels, such as a low density, high specific surface area, and high porosity,[1–4] and the unique features of native cellulose, such as hydrophilicity and biocompatibility.[5,6] These intriguing characteristics make cellulose aerogels potential substitutes for some petrochemicals in catalysts,[7] adsorbents,[8,9] fuel cells,[10,11] and thermal or electrical insulation materials.[12–14]

Cellulose aerogels are generally divided into regeneration cellulose aerogels and nanofibrillated cellulose (NFC) aerogels. In the preparation of regeneration cellulose aerogels, a procedure of dissolution, regeneration, and freeze drying or supercritical drying is frequently used.[15,16] Moreover, cellulose is difficult to hydrolyze or process in common aqueous or organic solvents because of its strong intermolecular and intramolecular hydrogen bonds, high degree of polymerization, and high degree of crystallinity[17]; thus, some special cellulose solvents, such as ammonium thiocyanate,[18] calcium and sodium thiocyanate,[19] lithium chloride/*N*,*N*-dimethyl acetamide,[20] ionic liquids,[21] and sodium hydroxide/poly(ethylene glycol) aqueous solutions,[22] are used during the aforementioned dissolution process. However, among cellulose solvents systems, numerous systems might cause serious environmental pollution. In comparison, the aerogels originated from NFC, whose preparation process mainly depends on the isolation of NFC and freeze-drying treatment, show considerable advantages from the perspective of environmental protection because no harmful solvents are required during NFC processing.[23] Furthermore, some time-consuming necessary courses, such as dissolution and gelation related to regeneration cellulose aerogels, are also not involved in preparation of NFC aerogels. Instead, some mild fast means, such as ultrasonic processing,[24] used for the isolation of NFC are used. Meanwhile, for NFC aerogels, the particular three-dimensional network formed by the self-assembly of NFCs with diameters of a few nanometers to several tens of nanometers also creates a large number of extraordinary performances in the density, adsorption, and conductivity.[25–28]

In this study, a mild method, which included chemical pretreatment, ultrasonic processing, solvent exchange, and *tert*-butanol (*t*-BuOH) freeze drying, for the preparation of ultralight NFC aerogels from NFC hydrocolloidal dispersions separated from coconut shell was examined. The as-prepared aerogels were

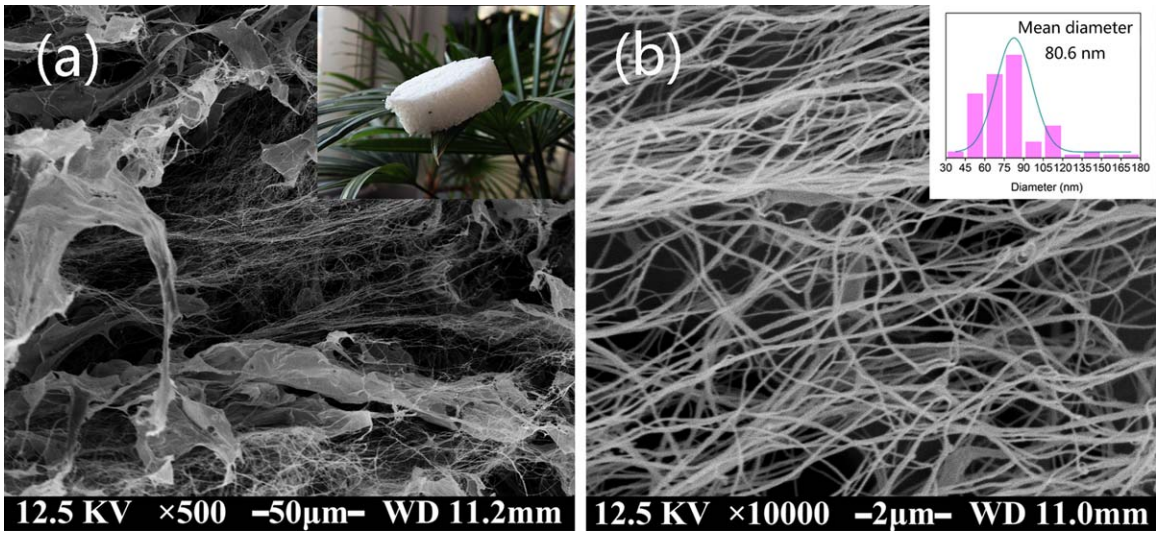

Figure 1. (a) Low- and (b) high-magnification SEM images of the NFC aerogels. The inset in panel a is a digital photograph of the lightweight NFC aerogels, and the inset in panel b presents the diameter distribution of the NFCs. [Color figure can be viewed in the online issue, which is available at wileyonlinelibrary.com.]

characterized with scanning electron microscopy (SEM), N_2 adsorption measurements, X-ray diffraction (XRD), and thermogravimetric analysis. Moreover, the NFC aerogels underwent hydrophobic modification by methyl trichlorosilane (MTCS) to improve the hydrophobicity and lipophilicity, and the interaction between the aerogels and modifying agent was investigated by Fourier transform infrared (FTIR) spectroscopy, and the modified samples were subsequently subjected to oil-adsorption and oil–water separation tests. Meanwhile, the adsorption properties of the modified aerogels for various organic solvents and oil were also investigated.

EXPERIMENTAL

Materials

Sixty-mesh powder of coconut shell after grinding and sieving was collected and dried *in vacuo* at 60°C for 24 h before used. All of the chemicals were supplied by Tianjin Kemiou Chemical Reagent Co., Ltd., and used without further purification.

Preparation of the NFC Aerogel

The purified cellulose from the coconut shell powder was a chemical pretreatment process, as referred to in our previous report.[29] Then, a certain amount of purified cellulose was uniformly dispersed in distilled water with magnetic stirring to form a 0.5 wt % aqueous dispersion, and the resulting mixture subsequently underwent an ultrasonic treatment for 60 min with an output power of 900 W in an ice–water bath. The ultrasonic process was performed at 20-25 kHz with a sonifier (JY99-IID, Scientz Technology, China) under a 50% duty cycle (i.e., a repeating cycle of 1-s ultrasonic treatment and 1-s shutdown). After ultrasonication, the suspension was run through a dialysis tubing cellulose membrane (average flat width = 76 mm, molecular weight cutoff = 14,000, Sigma–Aldrich) and underwent solvent exchange with *t*-BuOH by immersing the dialysis tubing in *t*-BuOH for 12 h. The obtained concentrated suspension, with a high viscosity and gel-like appearance, was freeze-dried at −35°C at 25 Pa

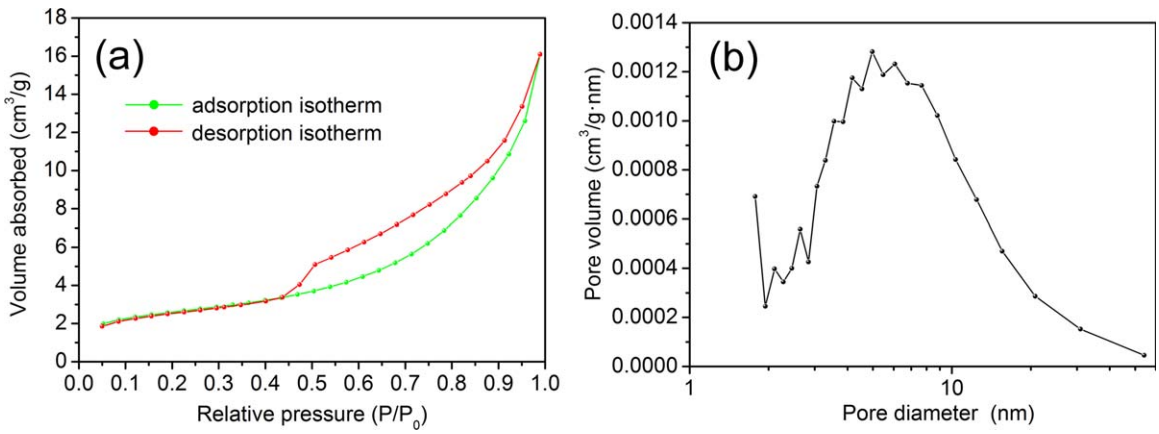

Figure 2. (a) N_2 adsorption−desorption isotherms and (b) pore diameter distribution of the NFC aerogels. P/P_0, where P is the equilibrium pressure and P_0 is the saturated equilibrium pressure. [Color figure can be viewed in the online issue, which is available at wileyonlinelibrary.com.]

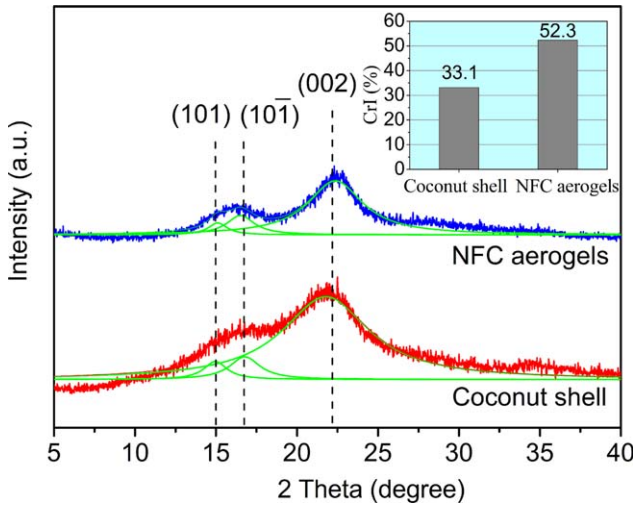

Figure 3. XRD patterns of the coconut shell and the NFC aerogels. The inset presents the crystallinity index (CrI) distributions. [Color figure can be viewed in the online issue, which is available at wileyonlinelibrary.com.]

for 48 h, and the resulting ultralight NFC aerogel was fabricated.

Hydrophobic Modification of the NFC Aerogel

The as-prepared NFC aerogel was hydrophobically modified with MTCS through a chemical vapor deposition method. A 5-mL beaker containing MTCS (300 μL) and NFC aerogels samples were placed in a sealed desiccator; we avoided direct contact between the samples and the modifying agent. Within the desiccator, the samples and volatile MTCS were allowed to react for 24 h at ambient temperature. This process successfully fabricated the hydrophobic aerogels.

Characterization

SEM observations were carried out on a FEI scanning electron microscope (Quanta 200). N_2 adsorption measurements were implemented by an accelerated surface area and porosimetry system (3H-2000PS2 unit, Beishide Instrument S&T Co., Ltd.). XRD patterns were run on an X-ray diffractometer (Rigaku D/MAX 2200) operating with Cu Kα radiation ($\lambda = 1.5418$ Å) at a scan rate (2θ) of 4°/min. The thermal stabilities were characterized with a thermogravimetric analyzer (TA, Q600) from 25 to 800°C with a heating rate of 10°C/min under a nitrogen atmosphere. The surface chemical compositions were investigated by an FTIR spectrophotometer (Magna 560, Nicolet, Thermo Electron Corp) in the range 650−4000 cm^{-1} with a resolution of 4 cm^{-1}. A contact angle analyzer (JC2000C) with a droplet volume of 5 μL was used to measure the water contact angle (WCA) of the samples.

RESULTS AND DISCUSSION

As shown in Figure 1(a), the NFC aerogels, with complex three-dimensional fibrillar networks, mainly consisted of interlaced tangled NFC aggregations (the slender filiform texture) and thin membranes possibly formed by a two-dimensional self-assembly of NFCs. At high magnification [Figure 1(b)], we observed that the slender NFCs were crosslinked and had a large length–diameter ratio; the diameters were within the scope of 30−180 nm, and the mean diameter of these NFCs was approximately 80.6 nm. Additionally, the NFC aerogels had an ultralow bulk density of 0.84 mg/cm^3, as determined by the weighed mass of aerogels divided by the measured volume. This was comparable to those of ultralight single-walled carbon nanotube aerogels (2.7 mg/cm^3),[30] *N*-doped graphene aerogels (2.1 mg/cm^3),[31] three-dimensional hierarchical boron nitride foam (1.6 mg/cm^3),[32] and periodic microlattice-constructed Ni foams (0.9 mg/cm^3)[33] and was slightly larger than those of ultraflyweight all-carbon aerogels (0.16 mg/cm^3),[34] the lowest density of ultralight materials ever reported. Furthermore, the NFC aerogels could stably stand on the leaf [inset in Figure 1(a)]; this further indicated the lightweight characteristics.

According to the N_2 adsorption measurements, the NFC aerogels showed a IV-type adsorption isotherm [Figure 2(a)], and the obvious hysteresis loop between the adsorption and desorption isotherms was formed by capillary condensation.[35] This indicated the presence of mesopores in the NFC aerogels. In addition, the pore diameter distribution curve in Figure 2(b) showed that the aerogels had pore sizes of 1−60 nm; this

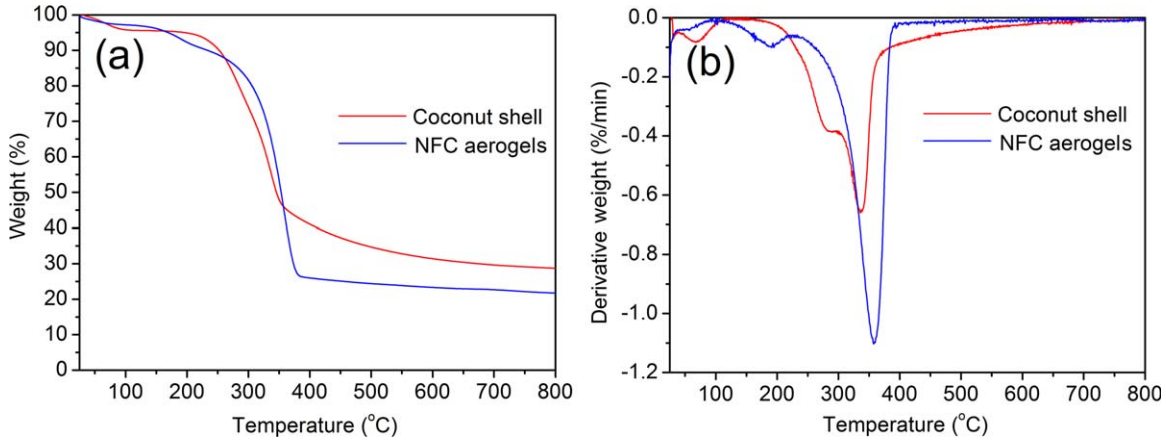

Figure 4. (a) TG and (b) DTG curves of the coconut shell and the NFC aerogels. [Color figure can be viewed in the online issue, which is available at wileyonlinelibrary.com.]

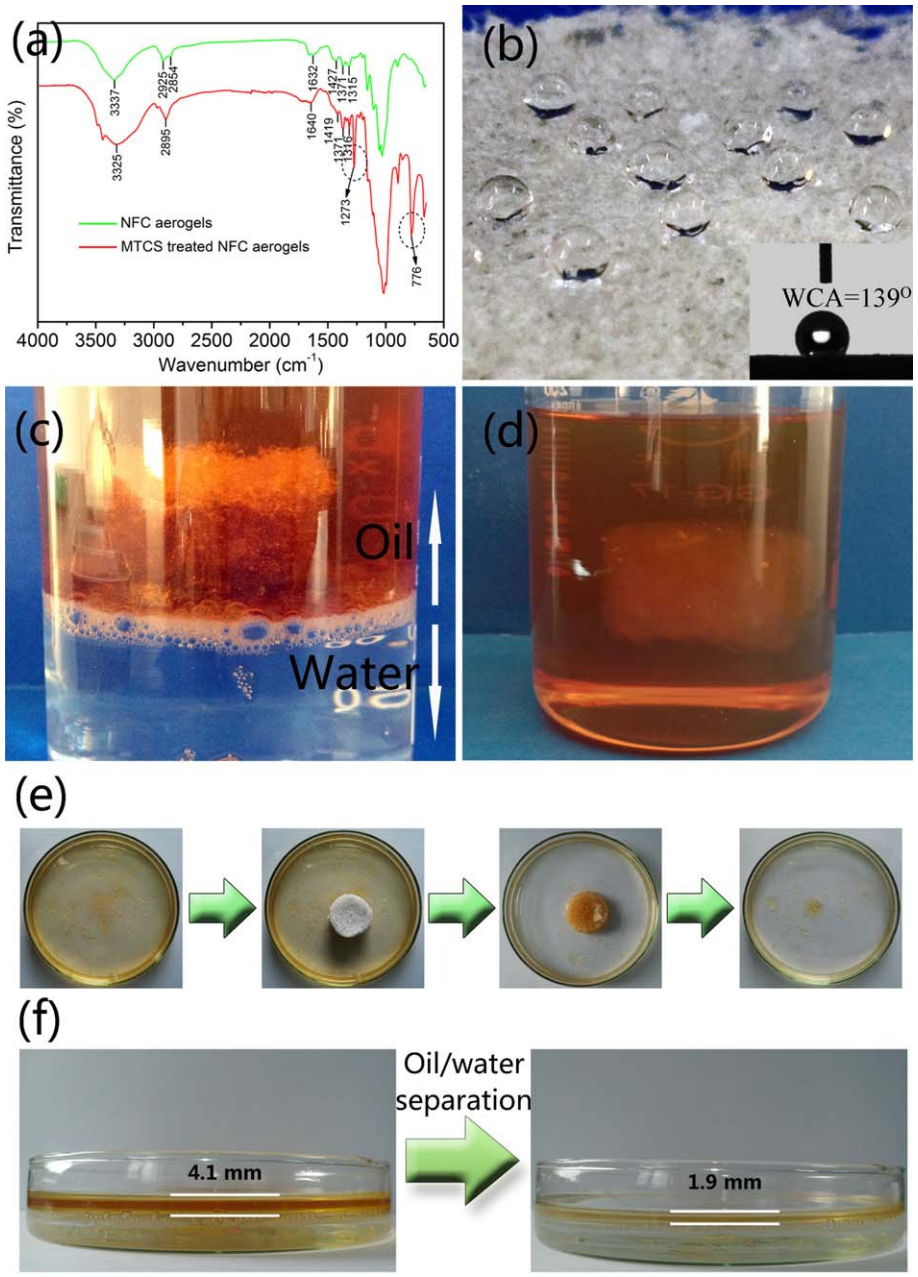

Figure 5. (a) FTIR spectra of the NFC aerogels and the MTCS-treated aerogels. (b) Water drops stability standing on the MTCS-treated aerogel surface. The inset presents WCA measurements. (c) MTCS-treated aerogel persistently staying in the oil layer instead of the water layer because of the water repellency properties. (d) Oil adsorption and (e) oil–water separation tests of the modified aerogel. (f) Oil layer thickness changes before and after the oil–water separation test. [Color figure can be viewed in the online issue, which is available at wileyonlinelibrary.com.]

further confirmed that the aerogels belonged to mesoporous materials. The Barrett–Joyner–Halenda and Brunauer–Emmett–Teller methods were carried out to calculate the pore characteristic parameters, and the results show that the samples had a specific surface area and pore volume of 9.1 m^2/g and 0.025 cm^3/g, respectively.

Figure 3 presents the XRD patterns of the coconut shell and the NFC aerogels. We observed that both samples exhibited typical cellulose I crystal structures with characteristic peaks around 15.1, 16.8, and 22.2°; these peaks corresponding to the (101), ($10\bar{1}$), and (002) planes[36] and revealed that the chemical pretreatment and ultrasonic processing did not change the crystal form. The inset in Figure 3 shows the crystallinity index distribution calculated by the Segal method.[37] Compared with the coconut shell, the crystallinity index of the NFC aerogels exhibited a significant improvement of 19.2% because of the removal of some amorphous substances, such as hemicellulose and lignin, during the chemical pretreatment,[38] and the improvement might also lead to the enhancement of the thermal stability.[39]

Figure 4 presents thermogravimetry (TG) and derivative thermogravimetry (DTG) plots of the coconut shell and the NFC aerogels. The slight mass loss for both samples before 150°C was due to the evaporation of retained moisture. For the coconut shell pyrolysis, in agreement with previous findings, the DTG curves displayed two main regions.[40,41] The first region (200−310°C) was mainly associated with the hemicellulose decomposition, which exhibited a pronounced shoulder; the second region (310−400°C) was related to the attainment of the maximum, principally because of cellulose degradation. This was followed by a rapid decay and a long tail. Moreover, lignin was the most difficult one to decompose among the three main components, whose decomposition happened slowly under the whole temperature range from ambient temperature to 800°C, and the wide range of temperatures also caused the absence of its characteristic peak. For the aerogels, because of the massive removal of amorphous substances, such as hemicellulose and lignin, there was only a severe decomposition stage of cellulose. For both samples, the degradation onset, 50% weight loss, and maximum degradation rate compared with those of the coconut shell (200, 345, and 349°C), the aerogel degradations all happened at higher temperatures (235, 353, and 357°C). This indicated the improvement of the aerogels' thermal stability.

The modification by MTCS contributed to the formation of a low-energy surface of the cellulose aerogels because of the replacement of surface hydrophilic hydroxyl groups on the cellulose with plentiful hydrophobic groups; this led to the generation of hydrophobicity.[42] Figure 5(a) presents the FTIR spectra of the NFC aerogels and the MTCS-treated aerogels. Evidently, the peaks in the two spectra were rather similar; particularly, the broad adsorption band centered around 3325 cm^{-1} was attributed to the O—H stretching. The peak at 2895 cm^{-1} was assigned to the C—H stretching; nevertheless, the NFC aerogels exhibited two peaks in this region (2915 and 2854 cm^{-1}); the peaks corresponded to the alkane C—H asymmetric and symmetric stretching vibrations, respectively. Moreover, the peaks around 1640, 1419, 1371, and 1316 cm^{-1} were derived from absorbed water, CH_2 symmetric bending, O—H bending, and C—H bending,[43] respectively. Apart from the similar peaks, the MTCS-treated NFC aerogels displayed two new strong peaks around 1273 and 776 cm^{-1}, which were attributed to the stretching vibrations of the Si—C bonds and the —CH_3 deformation vibrations of the siloxane compounds.[44] These confirmed the formation of the hydrophobic coating of MTCS on the NFC aerogels. As shown in Figure 5(b), the MTCS-treated NFC aerogels showed strong hydrophobic performance, with a WCA of 139°, and could stably hold water drops on the surface. Moreover, the modified aerogels persistently stayed on the oil layer and did not sink into the water layer under gravity after they were put into the oil–water mixture [Figure 5(c)]. This further suggested the generation of hydrophobicity. Subsequently, the modified aerogels were subjected to oil-adsorption tests by the immersion of the samples in diesel oil for 5 min [Figure 5(d)] and the weighing of the samples before and after the immersion. The result indicates that the aerogels exhibited a rapid adsorption rate and amazing oil adsorption properties (ca. 542 times the original dry weight) without any collapse in oil.

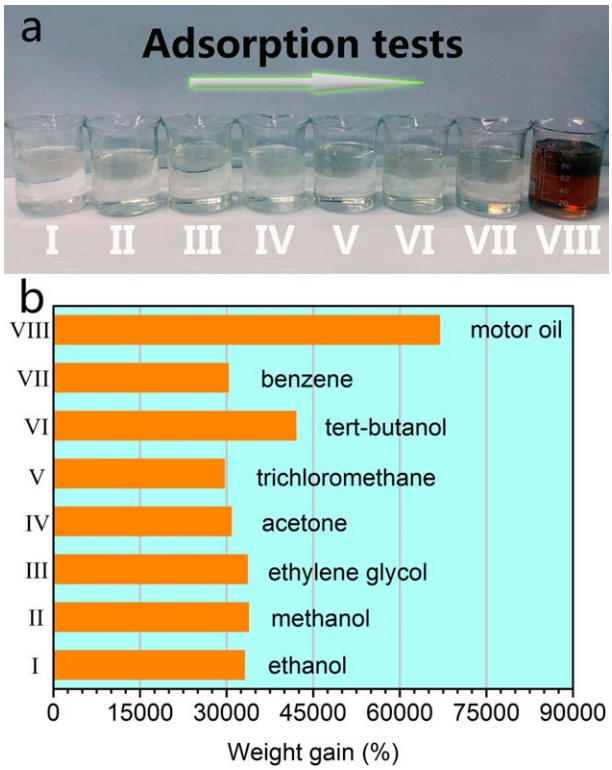

Figure 6. (a) Adsorption tests and (b) absorption efficiency of the MTCS-treated NFC aerogels for various organic liquids and oil. [Color figure can be viewed in the online issue, which is available at wileyonlinelibrary.com.]

Because of the excellent surface hydrophobicity and ultrastrong oil adsorption ability, the MTCS-treated NFC aerogels might be ideal candidates for the highly efficient separation–extraction of specific substances for oil spills. As shown in Figure 5(e), when a small piece of the aerogel was forced into the oil–water mixture, it could largely adsorb diesel oil instead of water. The whole process lasted 10 min, and the significant color difference before and after the test could be clearly distinguished; meanwhile, the oil layer thickness changed from 4.1 to 1.9 mm [Figure 5(f)], and this further demonstrated the superior oil–water separation performance of the aerogels.

The adsorption properties of the hydrophobic aerogels for some typical organic solvents and oil-like industrial alcohols (methanol, ethanol, etc.), aromatic compounds (benzene), and commercial petroleum products (motor oil), which are regarded as common pollutants in daily life or industry, were investigated [Figure 6(a)]. The absorption efficiency can be referred to as weight gain (weight percentage), defined as the weight of absorbed substances per unit weight of original NFC aerogel. The aerogels displayed ultrastrong absorption capacities for all of these organic liquids and oil, which could adsorb the liquids up to 296 to 669 times their own weights [Figure 6(b)], and the absorption efficiency was comparable with that of other high-performance adsorbing materials, such as carbon nanofiber aerogels (106−312 times),[45] ultraflyweight all-carbon aerogels (215−743 times),[34] and carbon nanotube/graphene oxide

aerogels (215−913 times).[46] This, thereby, indicated a facile, effective, and promising route for dealing with chemical leaks and oil spills. Nevertheless, because of the inferior flexibility, the aerogels had limited recyclability, and this defect could be improved in future work.

CONCLUSIONS

We prepared NFC aerogels with an ultralow bulk density (ca. 0.84 mg/cm^3) with coconut shell as the raw material after a mild, quick chemical pretreatment/ultrasonic processing/solvent exchange/*t*-BuOH freeze-drying process. The as-prepared aerogels, with their complex three-dimensional fibrillar networks, showed a cellulose I crystal structure and improved thermal stability compared with the coconut shell, and it had specific surface area and pore volume of 9.1 m^2/g and 0.025 cm^3/g, respectively. Moreover, the MTCS-modified NFC aerogels with highly hydrophobic properties (WCA = 139°) could adsorb 542 times the original dry weight of diesel oil, and they exhibited superior oil–water separation performances. Moreover, the hydrophobic aerogels also displayed a strong adsorption capacity for various organic solvents and oil (296−669 times the pristine weight). This, thereby, indicated a facile and useful route for dealing with chemical leaks and oil spills.

ACKNOWLEDGMENTS

This work was financially supported by the National Natural Science Foundation of China (contract grant number 31270590), a project funded by the China Postdoctoral Science Foundation (contract grant number 2013M540263), and the Doctoral Candidate Innovation Research Support Program of Science & Technology Review (contract grant number kjdb2012006).

REFERENCES

1. Liebner, F.; Haimer, E.; Potthast, A.; Loidl, D.; Tschegg, S.; Neouze, M.-A.; Wendland, M.; Rosenau, T. *Holzforschung* **2009**, *63*, 3.
2. Yang, W.; Wu, D.; Fu, R. *J. Appl. Polym. Sci.* **2007**, *106*, 2775.
3. Mihranyan, A. *J. Appl. Polym. Sci.* **2011**, *119*, 2449.
4. Sehaqui, H.; Salajková, M.; Zhou, Q.; Berglund, L. A. *Soft Matter* **2010**, *6*, 1824.
5. Tsioptsias, C.; Stefopoulos, A.; Kokkinomalis, I.; Papadopoulou, L.; Panayiotou, C. *Green Chem.* **2008**, *10*, 965.
6. Heath, L.; Thielemans, W. *Green Chem.* **2010**, *12*, 1448.
7. Xiong, R.; Lu, C.; Wang, Y.; Zhou, Z.; Zhang, X. *J. Mater. Chem. A* **2013**, *1*, 14910.
8. Gebald, C.; Wurzbacher, J. A.; Tingaut, P.; Zimmermann, T.; Steinfeld, A. *Environ. Sci. Technol.* **2011**, *45*, 9101.
9. Isobe, N.; Chen, X.; Kim, U.-J.; Kimura, S.; Wada, M.; Saito, T.; Isogai, A. *J. Hazard. Mater.* **2013**, *260*, 195.
10. Guilminot, E.; Fischer, F.; Chatenet, M.; Rigacci, A.; Berthon-Fabry, S.; Achard, P.; Chainet, E. *J. Power Sources* **2007**, *166*, 104.
11. Osman, M.; Shah, A.; Walsh, F. *Biosens. Bioelectron.* **2011**, *26*, 3087.
12. Tingaut, P.; Zimmermann, T.; Sèbe, G. *J. Mater. Chem.* **2012**, *22*, 20105.
13. Shi, J.; Lu, L.; Guo, W.; Zhang, J.; Cao, Y. *Carbohydr. Polym.* **2013**, *98*, 282.
14. Shi, J.; Lu, L.; Guo, W.; Sun, Y.; Cao, Y. *J. Appl. Polym. Sci.* **2013**, *130*, 3652.
15. Cai, J.; Kimura, S.; Wada, M.; Kuga, S.; Zhang, L. *ChemSus Chem* **2008**, *1*, 149.
16. Sescousse, R.; Gavillon, R.; Budtova, T. *Carbohydr. Polym.* **2011**, *83*, 1766.
17. Zhang, X.; Liu, X.; Zheng, W.; Zhu, J. *Carbohydr. Polym.* **2012**, *88*, 26.
18. Liu, C. K.; Cuculo, J. A.; Smith, B. *J. Polym. Sci. Part B: Polym. Phys.* **1989**, *27*, 2493.
19. Hattori, M.; Shimaya, Y.; Saito, M. *Polym. J.* **1998**, *30*, 49.
20. Dupont, A. L. *Polymer* **2003**, *44*, 4117.
21. Li, J.; Lu, Y.; Yang, D.; Sun, Q.; Liu, Y.; Zhao, H. *Biomacromolecules* **2011**, *12*, 1860.
22. Wan, C.; Lu, Y.; Jiao, Y.; Cao, J.; Li, J.; Sun, Q. *Mater. Sci. Technol.* to appear.
23. Dong, H.; Snyder, J. F.; Tran, D. T.; Leadore, J. L. *Carbohydr. Polym.* **2013**, *95*, 760.
24. Saito, T.; Kuramae, R.; Wohlert, J.; Berglund, L. A.; Isogai, A. *Biomacromolecules* **2012**, *14*, 248.
25. Valo, H.; Arola, S.; Laaksonen, P.; Torkkeli, M.; Peltonen, L.; Linder, M. B.; Serimaa, R.; Kuga, S.; Hirvonen, J.; Laaksonen, T. *Eur. J. Pharm. Sci.* **2013**, *50*, 69.
26. Carlsson, D. O.; Nyström, G.; Zhou, Q.; Berglund, L. A.; Nyholm, L.; Strømme, M. *J. Mater. Chem.* **2012**, *22*, 19014.
27. Cervin, N. T.; Aulin, C.; Larsson, P. T.; Wågberg, L. *Cellulose* **2012**, *19*, 401.
28. Aulin, C.; Netrval, J.; Wågberg, L.; Lindström, T. *Soft Matter* **2010**, *6*, 3298.
29. Li, J.; Wan, C.; Lu, Y.; Sun, Q. *Front. Agr. Sci. Eng.* **2014**, *1*, 46.
30. Jung, S. M.; Jung, H. Y.; Dresselhaus, M. S.; Jung, Y. J.; Kong, J. *Sci. Rep.* **2012**, *2*, 849.
31. Zhao, Y.; Hu, C.; Hu, Y.; Cheng, H.; Shi, G.; Qu, L. *Angew. Chem. Int. Ed.* **2012**, *124*, 11533.
32. Yin, J.; Li, X.; Zhou, J.; Guo, W. *Nano Lett.* **2013**, *13*, 3232.
33. Schaedler, T.; Jacobsen, A.; Torrents, A.; Sorensen, A.; Lian, J.; Greer, J.; Valdevit, L.; Carter, W. *Science* **2011**, *334*, 962.
34. Sun, H.; Xu, Z.; Gao, C. *Adv. Mater.* **2013**, *25*, 2554.
35. Wan, C.; Lu, Y.; Jiao, Y.; Jin, C.; Sun, Q.; Li, J. *Carbohydr. Polym.* **2014**, *118*, 115.
36. Oh, S. Y.; Yoo, D. I.; Shin, Y.; Kim, H. C.; Kim, H. Y.; Chung, Y. S.; Park, W. H.; Youk, J. H. *Carbohydr. Res.* **2005**, *340*, 2376.
37. Segal, L.; Creely, J.; Martin, A.; Conrad, C. *Text. Res. J.* **1959**, *29*, 786.

38. Fahma, F.; Iwamoto, S.; Hori, N.; Iwata, T.; Takemura, A. *Cellulose* **2011**, *18*, 443.

39. Assunção, R.; Vieira, J. G.; Meireles, C. D. S.; Cerqueira, D. A.; Silva Barud, H.; Ribeiro, S. J.; Messaddeq, Y. *Polym. Degrad. Stab.* **2007**, *92*, 205.

40. Grønli, M. G.; Várhegyi, G.; Di Blasi, C. *Ind. Eng. Chem. Res.* **2002**, *41*, 4201.

41. Yang, H.; Yan, R.; Chen, H.; Lee, D. H.; Zheng, C. *Fuel* **2007**, *86*, 1781.

42. Shewale, P. M.; Rao, A. V.; Rao, A. P. *Appl. Surf. Sci.* **2008**, *254*, 6902.

43. Lan, W.; Liu, C. F.; Yue, F. X.; Sun, R. C.; Kennedy, J. F. *Carbohydr. Polym.* **2011**, *86*, 672.

44. Shirgholami, M. A.; Shateri Khalil-Abad, M.; Khajavi, R.; Yazdanshenas, M. E. *J. Colloid Interface Sci.* **2011**, *359*, 530.

45. Wu, Z. Y.; Li, C.; Liang, H. W.; Chen, J. F.; Yu, S. H. *Angew. Chem. Int. Ed.* **2013**, *125*, 2997.

46. Pan, H.; Zhu, S.; Mao, L. *J. Inorg. Organomet.* **2014**, 1.